Faraday Discuss., 1997, **108**, 63–80

Concerted elimination dynamics from highly excited states

Qingguo Zhang,† Una Marvet and Marcos Dantus
Department of Chemistry, Michigan State University, East Lansing, Michigan 48824, USA

Photoinduced molecular detachment has been investigated for methylene iodide (CH_2I_2) and several related compounds (CH_2Br_2, CH_2Cl_2 and CF_2Br_2). Multiphoton excitation of these molecules at 310 nm gives rise to halogens in the D′ state. Femtosecond pump-probe experiments on the dissociation of these compounds indicate that the process is extremely fast (<60 fs) and proceeds without an intermediate. In addition to the characteristic D′ → A′ fluorescence at 342 nm, photodissociation of CH_2I_2 also produces several fluorescence bands in the 260–290 nm region. The CH_2I_2 transients show characteristic I_2 vibrational coherence. Time resolved data collected by detection at 272 nm also demonstrate clear, fast decaying rotational anisotropy, analysis of which reveals a distribution of rather high rotational levels of I_2. Based on analysis of the dissociation time, rotational anisotropy and vibrational coherence, and on the estimated partitioning of energy in the fragments, an I_2 concerted molecular detachment mechanism has been proposed.

1 Introduction

Understanding of molecular detachment processes represents an interesting and challenging area of research in the photodissociation research community. Processes of this type include, for example, the production of H_2 from photolysis of NH_3, H_2O and H_2CO molecules,[1] Cl_2 from $COCl_2$,[2] IBr from CH_2IBr[3] and I_2 from CH_2I_2.[4–10] Unlike most well known photodissociation processes, where dissociation involves only one bond, molecular detachment requires the breaking of more than one existing bond in addition to the formation of one or more new ones. Understanding of these processes thus presents a great challenge to both experimentalists and theoreticians, particularly following high energy excitation. In this paper, the femtosecond time resolved dynamics resulting from the photoinduced molecular detachment of Y_2 from CX_2Y_2 molecules (where X = H or F and Y = Cl, Br or I), are analysed with particular emphasis on the photodissociation of CH_2I_2.

Elimination of halogen molecules from dihaloalkanes has been investigated in several systems.[1–10] In general, this pathway is observed only at high excitation energies (>9 eV) and is usually a minor channel. Style and coworkers[4,5] were perhaps among the first to observe the 342 nm (D′ → A′) emission of I_2 resulting from photolysis of CH_2I_2 in the 125–200 nm vacuum ultraviolet region. Subsequent detailed analysis of the emission by Black[6] and Okabe *et al.*[7] revealed that the quantum yield for this channel is less than 1% at 123.6 nm. Weak I_2 emission bands in the 250–290 and 450–490 nm regions were also observed. The dissociation process $CH_2I_2 \rightarrow CH_2\ \tilde{X}(^3B_1) + I_2\ D'(^3\Pi_{2g})$ was found to involve an energy barrier of almost 1 eV. Fotakis *et al.*[8] observed I_2 fluorescence in the 260–290 and 300–340 nm regions by photodissociation of CH_2I_2 upon excitation with two 248 nm photons. Butler *et al.*[3] observed concerted elimination of the

† Present address: George R. Harrison Spectroscopy Laboratory, Massachusetts Institute of Technology, Cambridge MA, USA.

mixed halogen molecule IBr from excitation of CH_2BrI at both 210 nm and 193 nm. Their interpretation of the experimental data was that Rydberg and $n \rightarrow \sigma^*$ transitions were responsible for the IBr detachment at 193 and 210 nm, respectively.

Recently, Marvet and Dantus[10] conducted femtosecond pump–probe experiments on the photodissociation of CH_2I_2 to produce I_2. Coherent vibrational motion[11] of the nascent I_2 fragment was observed by monitoring depletion of the I_2 $D'(^3\Pi_{2g}) \rightarrow A'(^3\Pi_{2u})$ emission. It was determined in this experiment that the process resulting in the formation of I_2 is concerted; two possible mechanisms were proposed.

This study represents a continuation of our effort to elucidate the photoinduced molecular detachment mechanism of CH_2I_2 and related compounds. Dispersed fluorescence spectra following multiphoton excitation of CH_2I_2, CH_2Br_2, CF_2Br_2 and CH_2Cl_2 revealed the $D' \rightarrow A'$ fluorescence of the relevant halogen product in every case. In addition to the $D' \rightarrow A'$ fluorescence at 342 nm following dissociation of CH_2I_2, several I_2 fluorescence bands in the 260–290 nm region were also observed. By monitoring the emission at 272 nm from the I_2 photodissociation product, both coherent vibrational motion and rotational anisotropy were observed in the nascent I_2 fragment. Analysis of the observed vibrational coherence indicates which electronic state of I_2 produces the fluorescence at 272 nm. From the dissociation time of the molecule, the amount of kinetic energy in the fragments can be estimated. The I_2 detachment mechanism can then be inferred by consideration of the partitioning of energy in the fragments.

The paper will be organised as follows. In the following section a brief description of the experimental apparatus and techniques will be given. Presented in Section 3 are the dispersed fluorescence spectra and the time resolved transients resulting from the photodissociation of CH_2I_2, CH_2Br_2, CF_2Br_2 and CH_2Cl_2, along with analyses of these data. In Section 4, implications of the observed fast photodissociation, rotational anisotropy and vibrational coherence are discussed. Based on these discussions, a mechanism for the halogen detachment is proposed. Since the pump excitation involves a multiphoton transition, an extension of Baskin and Zewail's classical treatment of time dependent rotational anisotropy[12] to the case of multiphoton transitions has been implemented. A derivation of this is included in the Appendix.

2 Experimental

The experiments were performed using a femtosecond laser system capable of producing 60 fs pulses centered at 620 nm, with a pulse energy of 500 μJ, as described in refs. 10 and 13. Pump and probe pulses were prepared using a Mach Zhender interferometer. The beam in one arm of the interferometer was converted to 310 nm by second harmonic generation in a 0.1 mm potassium dihydrogen phosphate (KDP) crystal. Pump and probe beams were collinearly overlapped and focused in a quartz sample cell using a 200 mm focal length lens. Fluorescence from the product molecules was focused into a spectrometer.

All experiments were performed on neat vapour (1–10 Torr) of the relevant alkyl halide in a quartz cell (ice baths were used when necessary). Dehydrated sodium thiosulfate was used as a scavenger to prevent the accumulation of molecular halogens. The 310 nm (pump) pulse initiates the reaction by multiphoton excitation of the sample vapour. The dissociation products are detected by fluorescence. Spectra were taken using the 310 nm laser only and the wavelength scale was calibrated with Hg lamp emission. To obtain time resolved data, the probe pulse at 620 nm was used to deplete the population of halogen molecules in the fluorescent state and transients were recorded as a function of fluorescence signal *versus* time delay between pump and probe pulses. At each pump– probe time delay, the signal was collected for 10 laser shots; laser pulses with intensity more than one standard deviation from the mean were discarded. Typical transients contain data from 200 different time delays and are averages of 100 scans.

3 Results

3.A Dispersed fluorescence spectra

The dispersed fluorescence spectra resulting from multiphoton excitation of CH_2I_2, CH_2Br_2, CF_2Br_2 and CH_2Cl_2 at 310 nm are presented in Fig. 1 Fluorescence intensity has not been corrected for detection efficiency of the spectrometer. Most of the spectral features can be assigned to fluorescence from nascent halogen molecules resulting from the photodissociation. One of the most striking observations is that in all cases the principal fluorescent product is a halogen molecule in the D′ state.[14–17] It can be seen

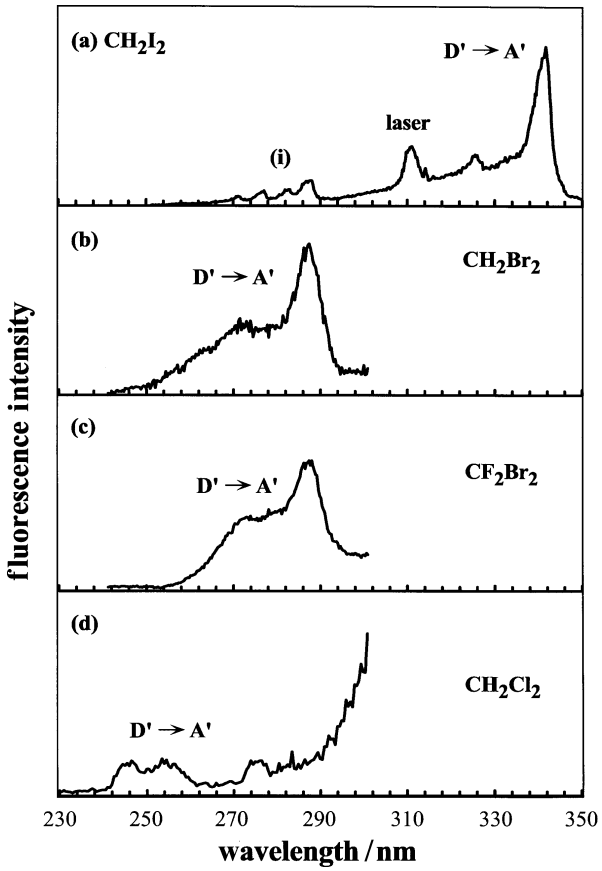

Fig. 1 Fluorescence spectra of diatomic halogens from multiphoton dissociation of haloalkanes at 310 nm. All spectra were obtained by gas-phase excitation at 310 nm in a static cell. (a) From CH_2I_2. The dominant fluorescence is from the I_2 D′ → A′ transition peaked at 342 nm. The region marked (i) corresponds to the f → A, F → X and f′ → B transitions. A small amount of laser scatter was observed at 310 nm. (b) From CH_2Br_2, showing the D′ → A′ fluorescence of Br_2. (c) From CF_2Br_2. The D′ → A′ spectrum of Br_2 is again observed. The product was found to be vibrationally colder than in CH_2Br_2. (d) From CH_2Cl_2. Again, a characteristic D′ → A′ fluorescence was observed, this time due to Cl_2. In this case the signal is weak. The increased signal from 280 towards 310 nm is due to laser scatter.

from the CH_2I_2 spectrum that there are also bands in the 260–290 nm region; the $f(^3\Pi_{0g+}) \rightarrow A(^3\Pi_{1u})$, $F(^1\Sigma_{0u}+) \rightarrow X(^1\Sigma_{0g+})$ and $f'(^1\Sigma_{0g+}) \rightarrow B(^3\Pi_{0u+})$ transitions of I_2 fluoresce in this region.[18,19] Comparison of the spectra produced from CH_2Br_2 and CF_2Br_2 shows that although in both cases Br_2 in the D′ state is a reaction product, there is a difference in the vibrational population. As expected, Br_2 formed from the dissociation of CF_2Br_2 is vibrationally colder. This is to be expected, since the difluoromethyl fragment, having a lower frequency bending mode, will absorb more of the available energy than the methyl radical upon detachment.

3.B Time-resolved data

Fig. 2 shows time resolved data obtained from the dissociation of CH_2I_2, CH_2Br_2, CF_2Br_2 and CH_2Cl_2. Each transient was obtained by multiphoton excitation at 310 nm, followed by depletion probing at 620 nm from the D′ state of the relevant diatomic

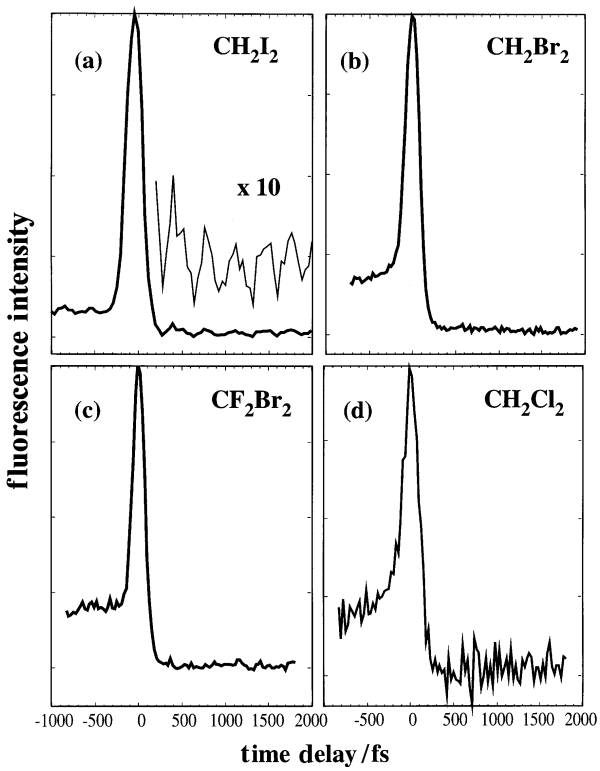

Fig. 2 Time resolved data from the multiphoton dissociation of alkyl halides at 310 nm followed by probing at 620 nm and detection of the D′ → A′ transition. (a) Dissociation of CH_2I_2 produces I_2. Dynamics of the nascent I_2 molecule are probed by depletion at 620 nm and detected by D′ state fluorescence at 340 nm. The large signal at time zero is a multiphoton effect (see text). The region to the left of time zero (negative time) is when the probe pulses arrive at the sample first. Vibrational oscillations are visible at positive time delays. This indicates that I_2 formation is concerted. (b) As with the CH_2I_2 data, the CH_2Br_2 transient shows depletion at positive times, and a strong time zero feature. Detection was at 287 nm. (c) The transient of CF_2Br_2 also shows depletion at positive times and a strong time zero feature. Again, detection was at 287 nm. (d) The CH_2Cl_2 signal is of low intensity and therefore noisy, but depletion by the 620 nm pulse at positive times is clear.

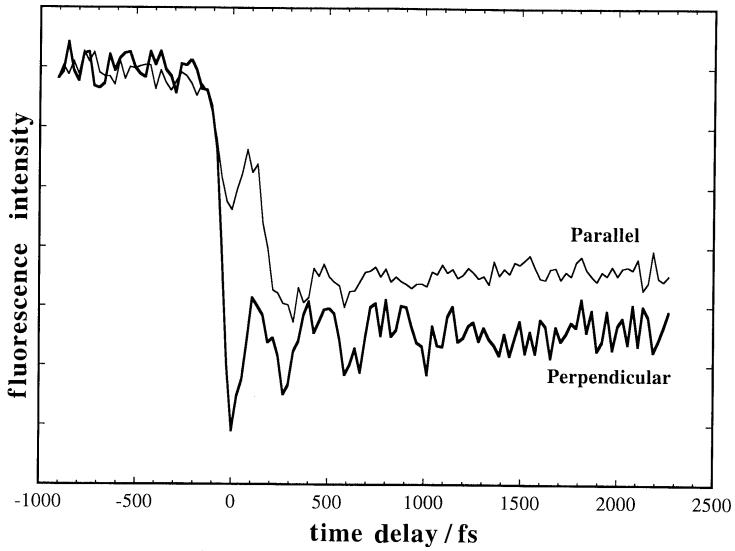

Fig. 3 CH_2I_2 pump-probe data recorded at 272 nm, corresponding to the f → A transition (see text). The data are plotted as a function of time delay between the pump (310 nm) and probe (620 nm) pulses and clearly show vibrational coherence. The transients were obtained for parallel and perpendicular polarization between pump and probe lasers. Differences between the two transients clearly indicate rotational anisotropy in the I_2 product.

halogen product. The polarisation of pump and probe pulses were aligned parallel to each other. Fluorescence was detected at the wavelength corresponding to the maximum intensity of the appropriate D′ → A′ transition. Fig. 2 shows that in each case, the fluorescence is depleted at positive times (probe pulse following pump, to the right of time zero). The intense features at time zero (pump and probe pulses overlapped in time) are due to a cooperative multiphoton effect which enhances the fluorescence signal. In this region, the molecule absorbs 310 nm photons and 620 nm photons simultaneously, which will enhance the fluorescence signal if it opens up another reaction pathway for the production of $Y_2(D')$. Because this process is only possible while the transition state exists, it is possible to determine a maximum dissociation time from the temporal width of this feature. The dissociation time of CH_2I_2 was found to be $\tau_{MeI_2} \leqslant 47$ fs,[13] indicating that elimination is prompt and that no intramolecular vibrational redistribution (IVR) takes place during dissociation. This was further confirmed by the dissociation time of *gem*-diiodobutane $C_3H_7CHI_2$, which was found to be $\tau_{BuI_2} \leqslant 87$ fs;[13] the increase can be completely accounted for by considering the difference in mass of the alkyl fragment. Fig. 2 also clearly shows vibrational coherence in the I_2 fragment. This is an indication that the process responsible for formation of the halogen molecules is concerted, since in-phase vibrations could not result unless the molecules formed within a short time of each other and on the same region of the product potential energy surface (PES). The observed oscillations were fitted to $v \approx 10$ of the I_2 D′ state.[13] While vibrational coherence in the Br_2 fragment has not to date been resolved, further efforts to do so are underway. The low signal to noise ratio in both the spectral and dynamic data from the CH_2Cl_2 sample is due to rather weak fluorescence from the nascent Cl_2 fragment.

In order to investigate the processes producing I_2 fluorescence in the 260–290 nm region, data were obtained from the CH_2I_2 sample by detection at 272 nm and at 285 nm. The dynamics observed for 285 nm detection are very similar to those found when

detecting the D′ → A′ transition (shown in Fig. 2). However, time resolved data collected at 272 nm was noticeably different, as can be seen in Fig. 3. At this wavelength there was no intense time zero feature, which indicates that there is no cooperative process available to produce I_2 in the state which fluoresces at 272 nm. The data shown in Fig. 3 were collected by setting the polarisation of the pump (310 nm) pulses to be normal to the optical table; the polarisation of the probe (620 nm) pulses was then aligned either parallel or perpendicular to the pump. Examination of the data reveals that depletion immediately after time zero is more efficient when pump and probe pulses are polarised perpendicular to each other than when they are parallel. This indicates that the dipole of the probe transition is perpendicular to the dipole of the pump transition at time zero. It is apparent from Fig. 3 that there is a considerable degree of anisotropy in the data, most of which decays during the first 500 fs after formation of the I_2 photodissociation product. The fast decay indicates a high degree of rotational excitation in the I_2 fragment. Although anisotropy was observed in the data collected at 340 nm, it was not sufficiently clear for rotational analysis because the large time zero feature overwhelms any fast dynamics nearby.

The time dependent rotational anisotropy is extracted from the data using the formula

$$r(t) = \frac{I_{\parallel} - I_{\perp}}{I_{\parallel} + 2I_{\perp}} \tag{1}$$

where $I_{\parallel}$ is the fluorescence intensity when pump and probe lasers are polarised parallel to each other and $I_{\perp}$ the intensity when they are perpendicularly polarised. This allows us to study the pure rotational dynamics, with no interference from vibrational oscillations. The experimental $r(t)$ curve is presented in Fig. 4. The average fluorescence intensity at negative time delay (probe earlier than pump) was subtracted from the parallel and perpendicular transients and proper normalisation of these transients at long time delay to their respective asymptotic limits was performed (see Appendix for

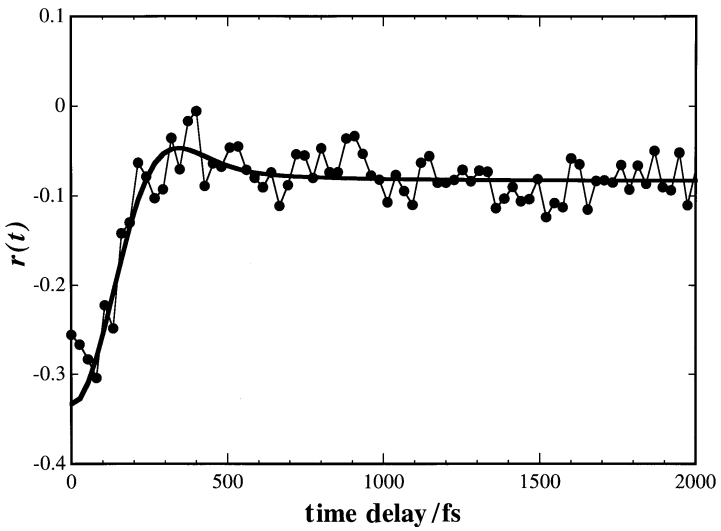

Fig. 4 Time resolved anisotropy, $r(t)$, obtained from the transients in Fig. 3. The experimental data were fitted by a least-squares algorithm taking into account the three photon excitation and the perpendicular orientation between pump and probe transition dipoles. Notice the anisotropy is close to $-1/3$ at time zero and reaches the asymptotic value of $-1/12$.

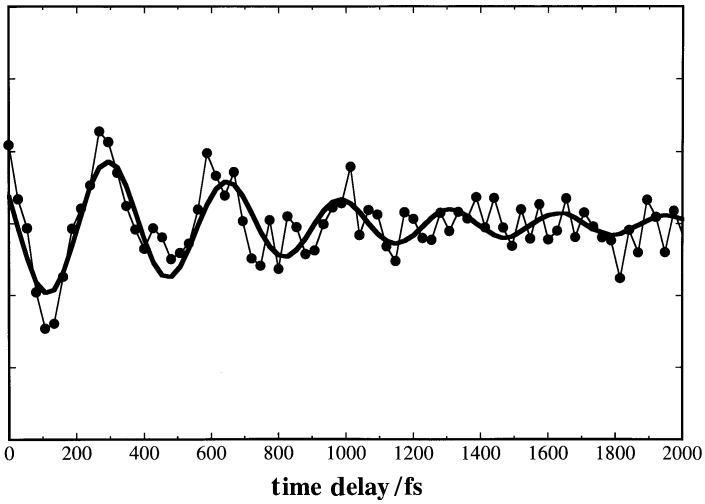

Fig. 5 Isotropic component ($I_{\parallel} + 2I_{\perp}$) of pump–probe data, showing the vibrational coherence at 272 nm in the I_2 product of CH_2I_2 photodissociation. The data were fitted using a least-squares procedure to obtain a Gaussian distribution of vibrational populations centered at $v \approx 11$ of the f state. This corresponds to an average period of 335 fs.

details). The observed data were not manipulated in any other way before evaluating $r(t)$. The observed $r(t)$ is modelled using the equation

$$r(t) = \frac{\sum_i P(j) r(j, t)}{\sum_j P(j)} \tag{2}$$

where the expression for $r(j, t)$ is given in Section 4C and $P(j)$ describes the rotational population of the I_2 fragment, in this case a Gaussian function given by

$$P(j) = \frac{1}{\sqrt{\pi}\Delta j} \exp\left[\frac{(j - j_{\max})^2}{(\Delta j)^2}\right] \tag{3}$$

Assuming a three photon excitation, a least-squares fit of the observed $r(t)$ data yields a rotational distribution having central value $j_{\max} = 354 \pm 38$ and a $1/e$ width $\Delta j = 509 \pm 52$.

In order to analyse the vibrational dynamics in the absence of rotational anisotropy the two transients were combined according to the formula[20]

$$I_{\text{isotropic}} = I_{\parallel} + 2I_{\perp} \tag{4}$$

The isotropic transient is shown in Fig. 5. The vibrational modulation in the data indicates that a significant portion of the iodine molecules resulting from this elimination channel are vibrating in phase. A least squares fit of the pure vibrational coherence was obtained using the spectroscopic parameters of the f state.[19] The observed dynamics were fitted to a Gaussian distribution of vibrational level population, centered at $v_{\max} \approx 11$.

3 Discussion

3.A Energetics for the elimination of halogen molecules

It is clear that the photodissociation pathways of dihaloalkanes leading to molecular halogen products require energies that are well above the thermodynamic threshold; for

CH_2I_2 the energy difference is approximately 5 eV.[6,7,21,22] This indicates that there are certain fundamental reasons why low energy excitation does not lead to molecular product formation. One of the reasons that has been advanced is based on the symmetry of the lower excited states of CH_2I_2. A dihaloalkane molecule CX_2Y_2 has C_{2v} symmetry (Fig. 6 shows the case for CH_2I_2, where X = H and Y = I). Transition dipole moments can therefore be parallel to the *X*, *Y* or *Z* directions (see Fig. 6). The UV absorption spectrum of CH_2I_2 has been deconvoluted into four bands, centered around 312, 286, 250 and 211 nm. These have been assigned to transitions to states having B_1, B_1, B_2 and A_1 symmetries respectively.[21,23,24] States with B_1 symmetry are expected to have a nodal plane between the iodine atoms, preventing the formation of molecular iodine products. Mixed alkyl halides, however, have been found to produce dihalogen products at lower excitation energies. Butler *et al.*[3] observed IBr from the photodissociation of CH_2BrI at 210 and 193 nm. The product was found to be IBr in the $^3\Pi_1$ state. No ground state product was observed. Because the symmetry of mixed dihaloalkanes is not C_{2v}, the symmetry constraints on the formation of molecular photoproducts discussed above are not applicable, which may account for the lower energy threshold and different electronic state of the dihalogen product.

Although symmetry considerations do not preclude the possibility of forming Y_2 as a photodissociation product from A_1 or B_2 states, little evidence of this pathway has been found upon excitation at 248 and 193 nm.[22] Pence *et al.* did find an unusual emission at 1.3 μm upon excitation of CH_2I_2 at 193 nm.[25] They attributed this to the formation of highly vibrationally excited I_2 in the $B(^3\Pi_{0u+})$ state, which would be expected to fluoresce at this wavelength.[26] If the 1.3 μm emission is indeed a result of this process, an alternative explanation for the apparent absence of molecular halogen products on photodissociation of CX_2Y_2 is that the lower electronic states are shallow compared to the excess energy available for the reaction. Therefore, although their formation is possible according to symmetry considerations, these products are not observed because they are formed with energies above their dissociation limit. In our experiments we observed no evidence of iodine products in any of the lower valence states (I_2 has a dissociation energy of *ca.* 1.5 eV in its ground state, *ca.* 0.5 eV in its B state and *ca.* 0.3

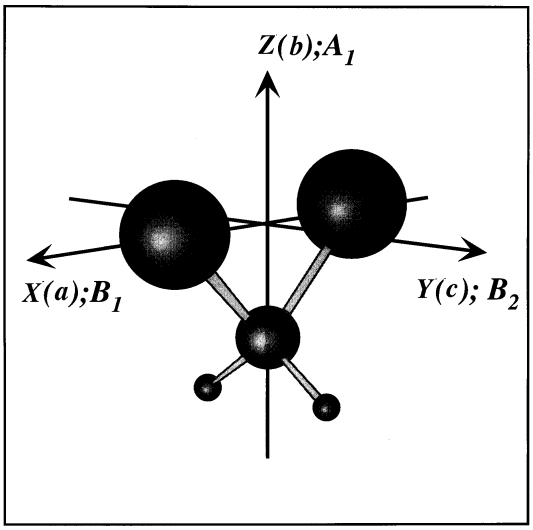

Fig. 6 3D model of a CH_2I_2 molecule, showing the principal (*X*, *Y*, and *Z*) and rotational axes (*a*, *b*, and *c*) as well as their transformation in C_{2v} symmetry. Notice that the center of mass is very close to the I–I axis.

eV in its A and A′ states). An ion-pair state, which correlates to $X^+ + X^-$, would be a good candidate for a dissociation product because these states are strongly bound. For halogens there are eighteen of these, corresponding to the ^3P, ^1D and ^1S terms of the X^+ ion. The thermodynamic threshold for the formation of iodine in the lowest energy ion-pair state, the D′ state, is 8.43 eV.[6,21,22,26] The threshold for observation of iodine in this state following the dissociation of CH_2I_2, measured by Okabe *et al.*, was found to be at 9.39 eV, indicating a 0.96 eV barrier.[7] Black found the threshold to be at 8.73 eV, indicating a lower barrier.[6] In either case, the elimination of I_2 from CH_2I_2 would require an excitation energy of more than 8.5 eV.

In an effort to elucidate the nature of the parent electronic state that correlates to dihalogen products, Okabe *et al.*[7] compared the absorption spectrum of CH_2I_2 in the vacuum ultraviolet region with the fluorescence excitation spectrum in the same region (342 nm detection). The absorption and fluorescence excitation spectra both showed broad continua, which were ascribed to C–I $\sigma \rightarrow \sigma^*$ transitions. Although features assignable to Rydberg transitions appeared in the absorption spectrum, their absence from the fluorescence excitation spectrum seems to exclude the involvement of Rydberg excitation in the I_2 photoinduced detachment process.

3.B Predominance of the D′ ion-pair state

In this section we focus on the predominance of the D′($^3\Pi_{2g}$) state. First tier ion-pair states have equilibrium energies within 0.16 eV of each other but they also have very different spectroscopic characteristics; for example the $E \rightarrow B$ transition occurs in the 400–436 nm region.[27] The two other ion-pair families are found approximately 0.9 and 1.5 eV higher. Three photon excitation with 310 nm is equivalent to 12 eV, which translates into an excess energy of 3 eV above the observed barrier to photoinduced molecular detachment at *ca.* 9 eV, thus bringing all the ion-pair states within energetic reach. The observed data for CH_2I_2 photodissociation indicates that only a small percentage (10%, not corrected for fluorescence yield or detection efficiency) of fluorescence occurs at wavelengths between 265 and 285 nm. These wavelengths correspond to the second tier of ion-pair states, which correlate with $X^+ (^3P_0) + X^-(^1S)$.[28] The observed predominance of the D′ state strongly suggests that electronic excitation directly correlates to this state.

The ion-pair states are known to be collisionally coupled to the D′ state,[14,29] but the mechanism for collisional coupling is not known. The collisional relaxation of many ion-pair states is extremely efficient, to the extent that it is used as the basis for the I_2 laser.[14] Perhaps the photodissociation process serves the role of a half-collision, thus forming primarily D′ products.

3.C The photodissociation mechanism

In this section, we will present a detailed analysis of the CH_2I_2 photodissociation process. As mentioned in Section 3.A, excitation of CH_2I_2 at 310 nm yields fluorescence bands that closely resemble the emission from the D′, F, f and f′ states of I_2. Thus the following discussion will only consider dissociation pathways leading to formation of these states. Since production of I_2 molecules in the D′, F, f and f′ states from a thermal sample of CH_2I_2 requires minimum energies of 8.38, 9.22, 9.20 and 10.2 eV respectively, at least three 310 nm photons are needed in each case to supply the necessary energy.[21,22] A four photon excitation would provide 16 eV of energy, which is far above the ionisation threshold of CH_2I_2, so we believe that a three photon excitation is more likely. Preliminary power dependence results also seem to support this conclusion. The following analysis is therefore made assuming that the excitation is a three photon process.

If a 12 eV excitation produces I_2 in the D′, F, f and f′ states, only the three lowest electronic states of CH_2, *i.e.* $\tilde{X}(^3B_1)$ ($T_0 = 0.0$ eV), $\tilde{a}(^1A_1)$ ($T_0 = 0.39$ eV), and $\tilde{b}(^1B_1)$ ($T_0 = 1.27$ eV), can be produced by the photodissociation process. Table 1 lists the possible combinations of the I_2 and CH_2 states, each of which represents a distinct photodissociation channel of CH_2I_2. For each channel, Table 1 also presents the minimum energy required for the dissociation process, and the remaining energy available for internal and kinetic energy of the fragments.

To understand the photodissociation process properly, we must first gain an understanding of how internal energy in the parent molecule becomes distributed in the fragments. Most of the rotational energy about the Z axis, the symmetry axis of CH_2I_2, remains as rotational energy in the I_2 fragment because the moment of inertia of I_2 is significantly larger than that of CH_2 (see Fig. 6 for definition of the axes). Because the center of mass of CH_2I_2 is extremely close to the iodine atoms, rotational motion of CH_2I_2 about the X axis will be manifested as translational motion of the CH_2 fragment, while rotational motion about the Y axis will be partitioned upon dissociation into I_2 rotation and CH_2 translation. Thus CH_2 gains some translational energy from the dissociation process but the I_2 fragment essentially gains no translational motion in the center–of–mass frame.

To estimate the amount of available energy that is partitioned into center-of-mass translational motion of the fragments we use a dissociation time of 47 fs for the dissociation of CH_2I_2 as an upper limit.[19] Assuming an exponential form of repulsive potential with a $^1/e$ length parameter L, the estimated dissociation time $\tau_{1/2}$ can be related to the amount of translational energy E as follows:

$$\tau_{1/2} = L\sqrt{\left(\frac{\mu}{2E}\right)}\ln\left(\frac{4E}{\gamma}\right) \tag{5}$$

where γ is the half-width of the energy distribution of the probe pulse (0.0125 eV for the 620 nm pulses) and μ is the reduced mass of the CH_2 and I_2 products, assuming they form a pseudodiatomic (essentially the mass of the CH_2 fragment). Using a length parameter of $L = 0.35$ Å, which has been found for CH_3I,[31,32] the translational energy is estimated to be 1.4 eV.

A quantitative evaluation of the partitioning of parent rotational energy can to some extent be determined indirectly, from analysis of the rotational anisotropy of the fragments. Since clear rotational anisotropy was observed only for I_2 fluorescence at 272 nm, the following discussion will concentrate on this region.

Table 1 Possible combinations of I_2 and CH_2 states

I_2 states	CH_2 states	energy required/eV[21,22]	available energy/eV
$D'(^3\Pi_{2g})^{14}$	$\tilde{X}^3B_1$	8.38	3.62
	$\tilde{a}^1A_1$	8.77	3.23
	$\tilde{b}^1B_1$	9.65	2.35
$F(^1\Sigma_{0u^+})^{15}$	$\tilde{X}^3B_1$	9.22	2.78
	$\tilde{a}^1A_1$	9.61	2.39
	$\tilde{b}^1B_1$	10.49	1.51
$f(^3\Pi_{0g^+})^{19}$	$\tilde{X}^3B_1$	9.20	2.80
	$\tilde{a}^1A_1$	9.59	2.41
	$\tilde{b}^1B_1$	10.47	1.53
$f'(^1\Sigma_{0g^+})^{19}$	$\tilde{X}^3B_1$	10.2	1.8
	$\tilde{a}^1A_1$	10.6	1.4
	$\tilde{b}^1B_1$	11.5	0.5

Fig. 4 shows anisotropy data collected at 272 nm for dissociation of CH_2I_2. Analysis of these data using a simple one photon pump and probe model for $r(t)$ failed to reproduce the experimentally observed value at time zero; one can see from Fig. 4 that the $r(t)$ value at time zero is close to -0.3 rather than the expected value of -0.2 for a situation where pump and probe transition dipoles are perpendicular to each other. Although one can simply dismiss this discrepancy based on the level of signal to noise ratio, we suspect that it is caused by the multiphoton nature of our pump transition. A three photon pump transition would be expected to produce a greater degree of alignment than is expected for a single photon transition because it produces a $(\cos\theta)^6$ distribution in the nascent products rather than a $(\cos\theta)^2$ distribution.[33] The narrower initial alignment causes the dephasing of rotational anisotropy to appear faster than it really is. In order to model time-dependent rotational anisotropy experiments in which the excitation is a multiphoton process, we extended the classical treatment by Baskin and Zewail[12] (detailed derivation given in the Appendix).

For an m-photon pump and one photon probe experiment, if all the pump transition dipoles are aligned parallel to each other, we find that the rotational anisotropy can be expressed simply as follows:

$$r(j, t) = \frac{2m}{2m + 3} \langle P_2[\cos \eta_j(t)] \rangle \tag{6}$$

where $\eta_j(t)$ is the time-dependent angle between the pump transition dipole at time zero and the evolving direction of the probe transition dipole of the product. $P_2(x) = (3x^2 - 1)/2$ is the second order Legendre polynomial. The average is over the rotational degrees of freedom of the photodissociation product being probed. When the pump transition dipole is parallel to the probe dipole at time zero, one can specialize eqn. (6). Assuming that the product is a linear species and that its electronic and spin angular momenta can be neglected, one finds

$$r_{\parallel,\parallel}(j, t) = \frac{m}{2(2m + 3)} (1 + 3 \cos 2\omega_j t) \tag{7}$$

where $\omega_j = 4\pi Bj$ denotes the j-dependent nutational frequency of the fragment being probed. B is the rotational constant of the fragment. Similarly, for the situation where the pump and probe dipoles are perpendicular to each other at time zero, one obtains

$$r_{\parallel,\perp}(j, t) = -\frac{m}{4(2m + 3)} (1 + 3 \cos 2\omega_j t) \tag{8}$$

Application of eqn. (8) to our case, *i.e.* a three-photon pump with perpendicular pump–probe dipole orientation, gives rise to the following expression for the j-averaged rotational anisotropy:

$$r_{\parallel,\perp}(t) = -\frac{1}{12} - \frac{1}{4} \frac{\sum_j P(j) \cos 2\omega_j t}{\sum_j P(j)} \tag{9}$$

Here $P(j)$ stands for the relative population of level j. It is obvious from eqn. (9) that $r(0) = -\frac{1}{3}$, which is in close agreement with the observed value (see Fig. 4). We have fitted the observed rotational anisotropy data shown in Fig. 4 to eqn. (9). The best least-squares fit is found for a rotational distribution centered at $j_{max} = 354 \pm 38$, and width $\Delta j = 509 \pm 52$. This implies that the average rotational energy of the product I_2 molecules is 0.3 eV.

To facilitate the discussion, Table 2 lists certain structural and spectroscopic information for CH_2I_2, CH_2 and I_2. As we can see, the B and C rotational constants of the CH_2I_2 ground state are very similar to the B rotational constant of I_2, with a value of

Table 2 Structural and spectroscopic data for CH_2I_2, CH_2 and I_2

	R_{I-I}/Å	ω_{I-I}/cm^{-1}	HCH/degrees	ω_{HCH}/cm^{-1}	A/cm^{-1}	B/cm^{-1}	C/cm^{-1}
CH_2I_2 X	3.579[b]		112.7		0.710	0.020	0.019
CH_2 $\tilde{X}$[c]			134.0	963.1	73.81	8.45	7.18
CH_2 $\tilde{a}$[c]			102.4	1352.6	20.14	11.16	7.06
CH_2 $\tilde{b}$[c]			140	357		7.57	
I_2 D′[15]	3.5944	103.960				0.020563	
I_2 F[d]	3.596	96.313					
I_2 f[19]		104.1447					
I_2 f′[19]		96.980					

[a] Values calculated by the HF/3-21G method. [b] Z. Kisiel, L. Pszczólkowski, W. Caminati and P. G. Favero, *J. Chem. Phys.*, 1966, **105**, 1778. [c] G. Herzberg, *Molecular Spectra and Molecular Structure III*, Reprint edition, Krieger, Malabar 1991. [d] T. Ishiwata, T. Kusayanagi, T. Hara and I. Tanaka, *J. Mol. Spectrosc.* 1986, **119**, 337.

approximately 0.02 cm^{-1}. This gives a Boltzmann distribution at room temperature centered at $j \approx 90$. Thus for a room temperature sample of CH_2I_2, the average rotational quantum number is expected to be of the order of 100. This is much smaller than the measured rotational distribution of the I_2 products. Conservation of angular momentum demands that the difference, about 250 $\hbar$, be taken up by the CH_2 fragment.

The rotational excitation of the I_2 fragment can be accounted for if one of the two C—I bond breaking processes happens faster than the other. This would exert a large torque on the fragments, causing them to exhibit counter rotation and a high degree of rotational excitation. The strong torque and available excess energy would break the second C—I bond within 50 fs of the first. This corresponds to the concerted sequential mechanism shown in Fig. 7. By contrast, if the photodissociation process proceeded by the concerted simultaneous mechanism, one would not expect to observe rotational excitation in either fragment.

If all of the 250 $\hbar$ of angular momentum were to go into the rotation of the CH_2 fragment, a simple BJ^2 argument predits that the amount of rotational energy would be of the order of 60 eV! This is clearly impossible; in fact, much of the torque exerted on CH_2 will cause translational excitation. The 250 $\hbar$ deficit in angular momentum must then be accounted for by a non-zero impact parameter b using $\boldsymbol{L} = \mu v b$, where v is the relative velocity of the fragments. Assuming an impact parameter of 2 Å, the translational energy of the CH_2 fragment can be estimated to be 2.3 eV. On the other hand, if we assume an impact parameter of 3 Å, the estimated CH_2 translational energy would be 1.0 eV. Thus the estimated translational energy is very sensitive to the impact parameter, a quantity that depends critically upon the details of the dissociation mechanism, such as at what point the second C—I bond breaks and in which direction the two fragments fly apart. If comparison is made with the previous 1.4 eV estimation of the CH_2 translational energy, we find that the impact parameter is approximately 2.6 Å.

Since the I—I interatomic distance in ground state CH_2I_2 is rather close to the bond lengths in the D′, F, f and f′ states of the I_2 molecule, significant vibrational excitation in the I_2 fragment is not expected. However, because the HCH angle in ground state CH_2I_2 differs significantly from the bond angle of CH_2, particularly in the $\tilde{X}$ and $\tilde{b}$ states, vibrational excitation should be expected in the CH_2 photofragment. This could represent a significant amount of energy, especially when one considers the high vibrational frequencies in CH_2 electronic states.

For most of the pump–probe data we collected, only a few vibrational oscillations were observed (see Fig. 5). It is not certain whether one could observe more if the signal-to-noise ratio was improved, or whether the dephasing is due to the nature of the

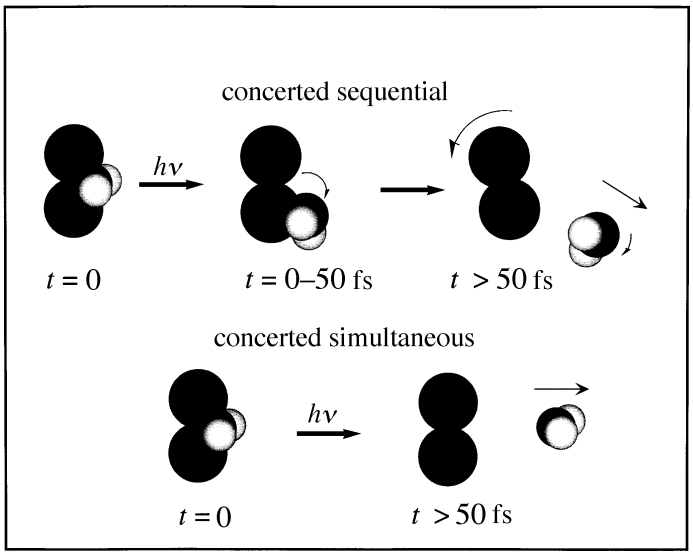

Fig. 7 Schematic diagram of possible reaction mechanisms for the photoinduced molecular detachment of I_2 from CH_2I_2. Two concerted processes are depicted. In the concerted sequential mechanism the first carbon–iodine bond breaks and an iodine–iodine bond is formed while the second iodine is still attached to the carbon. This first step imparts a large torque on the CH_2 fragment. Subsequent breaking of the second carbon–iodine bond completes the reaction. This mechanism produces iodine molecules with a high degree of rotational angular momentum (see text). The time scales given for this process are based on our experimental results. The concerted simultaneous mechanism involves the breaking of the two carbon–iodine bonds simultaneously with formation of an iodine–iodine bond. This would be expected to produce molecular iodine products with very little rotational angular momentum in direct contrast to our experimental findings.

nascent vibrational population. For the present, we will simply model the vibrational motion of the I_2 fragment as a classical anharmonic oscillator with the observed dephasing accounted for by anharmonicity. Assuming a Gaussian distribution of vibrational level populations, a least squares fit to the pure vibrational coherence data yields the fit shown in Figure 5. The fit was obtained using a vibrational level distribution that is centered around $v = 11$ of the I_2 f state. Fits were also attempted using the parameters of the F and f′ states, but did not match the data as well. This suggests that the fluorescence detected at 272 nm originates from the f → A transition.

If the above arguments are correct, the fragments contain at least 1.7 eV of translational and rotational energies. Therefore, if we assume that excitation is a three-photon process and that I_2 is formed in the f state, the formation of CH_2 ($\tilde{b}$) can be ruled out because there is not enough energy available (see Table 1). If this is the case, we are left with two choices, *i.e.* CH_2 ($\tilde{X}$) + I_2 (f) and CH_2 ($\tilde{a}$) + I_2 (f). Which of the two channels is responsible for photodissociation of CH_2I_2 to yield I_2 fluorescence at 272 nm remains to be investigated. Thus, much of the following discussion is meant to be taken more as speculation than as matter of fact.

Fig. 3 clearly shows that there is a high degree of anisotropy as a result of the CH_2I_2 photodissociation process. If each of the transition dipoles corresponding to the three photon pump transition had different orientations, one would not expect the anisotropy to be so clear.[33] Thus, the three transition dipoles are likely to be parallel to each other, particularly when excitation is by a femtosecond pulse because this is the most favourable situation for absorption. Since CH_2I_2 absorbs at 310 nm and leads to a B_1 state,[21] one expects resonance enhancement if the three photon process involves the B_1 state as

the first transition. If this is the case, the dissociative state reached is expected to be a B_1 electronic state at about 12 eV above the ground state. A B_1 transition in this molecule is aligned along the I–I direction (see Fig. 6); in this case the probe transition would be perpendicular to the I_2 bond. However, as we have already discussed, formation of I_2 from a B_1 state of CH_2I_2 is symmetry forbidden. It is also possible that there is a two − photon resonance enhancement transition from the ground state, in which case A_1 (parallel to the Z axis) and B_2 (perpendicular to the CH_2 plane) symmetries would be allowed as well.

It is possible that the molecular detachment proceeds by a charge transfer type mechanism such that one of the iodine atoms gains electron density while the other loses it. The electron density redistribution would have the effect of generating a Coulombic attraction between the two iodine atoms while at the same time weakening the two C—I bonds. This is also supported both by the fact that the halogen states that have been observed are all ion-pair, *i.e.* charge transfer, states and that molecular dissociation products are not observed until the excitation energy approaches the ionisation threshold of the molecule.

To summarise the above discussion, we can construct the following picture about how we think of the photodissociation process of CH_2I_2 at an excitation energy of 12 eV. A three (310 nm) photon transition excites CH_2I_2 molecules from the thermally populated ground electronic state to a dissociative state; the transition may be of a charge transfer type. One of the C—I bonds breaks and a bond forms between the two iodine atoms (see concerted sequential mechanism in Fig. 7); this generates an enormous amount of torque on the CH_2 and I_2 moieties to tear the second C—I bond apart. Dissociation occurs within 50 fs of the initial excitation. The remaining energy from the 12 eV initially deposited in the CH_2I_2 molecule is distributed between the photofragments in the following fashion. The CH_2 fragment gains a tremendous amount of translational energy and a sizeable degree of vibrational excitation but little rotational or electronic excitation. On the other hand, the I_2 fragment is left in a highly excited electronic state with a large amount of rotational excitation but only moderate vibrational excitation and very little translational energy. This mechanism is quite in keeping with the mechanism proposed by Hoffmann and coworkers,[9] although the latter was proposed for CX_2Y_2 dissociation from low-energy potential surfaces. The concerted simultaneous mechanism shown in Fig. 7 would not yield the high rotational energies observed experimentally.

4 Conclusions

Molecular halogen detachment processes have been investigated for methylene iodide and some related haloalkanes. It was found that multiphoton excitation of these molecules at 310 nm gives rise in every case to halogen molecules in the D′ state. Femtosecond time-resolved experiments performed on these dihaloalkanes show that the photoinduced molecular detachment processes are extremely fast (<60 fs). Selective detection of fluorescence from CH_2I_2 photodissociation products at 340 nm, 286 nm and 272 nm reveals characteristic I_2 vibrational coherence, indicating that the reaction mechanism is concerted. The 272 nm transients also clearly demonstrate fast decaying rotational anisotropy.

Least squares fit of the anisotropy to a Gaussian distribution of rotational level occupations reveals a distribution of rather high I_2 rotational levels, with the distribution center at around $j = 350$ and a width of $\Delta j = 500$. This high degree of rotational excitation has been explained by invoking the following so-called concerted sequential I_2 detachment mechanism (see Fig. 7). When CH_2I_2 is excited to a highly electronically excited dissociative state, one of the two C—I bonds breaks and an I—I bond forms. Then the second C—I bond ruptures, leaving rotationally excited I_2 and translationally

hot CH_2 fragments. This occurs within 50 fs of the initial excitation. The high degree of rotational excitation in the I_2 product rules out the concerted simultaneous mechanism shown in Fig. 7 as a possible reaction pathway; if this were the process that occurs, C_{2v} symmetry would be maintained throughout the dissociation and there would be no rotational excitation in either fragment.

Although the 272 nm fluorescence resulting from excitation of CH_2I_2 can in principle be attributed to emission from any of three ion-pair states of I_2 (F, f, or f′), analysis of the vibrational coherence at this wavelength suggests that the $f \rightarrow A$ transition is the source of this fluorescence. The electronic state of the CH_2 fragment has been determined to some extent for this particular dissociation channel by energetic considerations. Assuming three-photon excitation of CH_2I_2 and taking into consideration the high translational energy imparted into the CH_2 fragment and the relatively high rotational energy in the I_2 fragment, we have argued that the CH_2 fragment is likely to be in its ground ($\tilde{X}$) or first excited ($\tilde{a}$) electronic state. Time-of-flight mass spectrometry following photodissociation of CH_2I_2 in the molecular beam will allow us to analyse the final electronic state of the CH_2 fragments. Future experiments on CF_2I_2 will also allow us to obtain electronic and vibrational information by detection of the UV fluorescence of the CF_2 fragment.

We would like to thank Professor S. Stolte and Dr S. Baskin for helpful discussions. This work was partially supported by a Camille and Henry Dreyfus New Faculty Award. M.D. is a Beckman Young Investigator and a Packard Science and Engineering Fellow.

Appendix

In this appendix, a brief formulation of the rotational anisotropy

$$r(t) = \frac{\sum_j P(j) r(j, t)}{\sum_j P(j)} \tag{A1}$$

will be presented for experiments with an m-photon pump transition and one-photon probe. In eqn. (A1), $r(j, t)$ is the anisotropy specific to a particular j level with population $P(j)$ of the fragment being probed. The following derivation assumes that all dipoles of the pump transition are parallel to each other. Extension of eqn. (8) from Baskin and Zewail[12] to such cases, gives

$$I_\delta(j, t) \propto \langle [1 + 2P_2(\cos \alpha)]^m [1 + 2P_2(\cos \delta) P_2[\cos \eta_j(t)] P_2(\cos \alpha)] \rangle \tag{A2}$$

where α denotes the angle between the polarization of the pump pulse and the pump transition dipole, δ the angle between the pump and probe polarizations and $\eta_j(t)$ the angle between the pump and the probe transition dipoles. Since the probe dipole rotates with the fragment being probed, $\eta_j(t)$ is dependent on the rotational quantum number j and is a function of time. The average is over certain rotational degrees of freedom, such as the angle α. The second order Legendre polyomial $P_2(x) = (3x^2 - 1)/2$.

Note that $1 + 2P_2(\cos \alpha) = 3 \cos^2 \alpha$. Thus, raising the first term in eqn. (A2) to the power of m accounts for the transition probability of the m-photon pump excitation. Substituting $\xi = P_2(\cos \delta) P_2[\cos(\ _j(t)]$, which is independent of α, eqn. (A2) can be recast as

$$\begin{aligned} I_\delta(j, t) &\propto \frac{1}{2} \int_0^\pi d\alpha \sin \alpha [1 + 2P_2(\cos \alpha)]^m [1 + 2\xi P_2(\cos \alpha)] \\ &= a + b\xi \end{aligned} \tag{A3}$$

where the average over α in eqn. (A2) is now explicit. The integral yields two terms, one of which is linear with ξ and the other independent of it. The coefficients a and b can be evaluated in terms of m:

$$a = 2\,\frac{3^m}{2m+1}$$

$$b = 8m\,\frac{3^m}{(2m+1)(2m+3)} \tag{A4}$$

When the polarisations of pump and probe are parallel to each other $d = 0$, which gives $P_2(\cos\delta) = 1$. When the pump and probe are polarised perpendicular to each other, on the other hand, we have $\delta = \pi/2$ and $P_2(\cos\delta) = -1/2$. Recalling that $I_\delta = a + b\xi$ and $\xi = P_2(\cos\delta)P_2(\cos\eta)$, the result is

$$I_{\parallel}(j, t) \propto a + bP_2[\cos\eta_j(t)]$$

$$I_{\perp}(j, t) \propto a - \frac{b}{2}\,P_2[\cos\eta_j(t)] \tag{A5}$$

The time-dependent anisotropy is then obtained by substitution of eqn. (A5) into eqn. (A1) to give

$$r(j, t) = \frac{b}{2a}\,\langle P_2[\cos\eta_j(t)]\rangle = \frac{2m}{2m+3}\,\langle P_2[\cos\eta_j(t)]\rangle \tag{A6}$$

For the case of $m = 1$, *i.e.* one-photon pump and one-photon probe, (A6) reduces to the well known expression for $r(t)$.[12] It is interesting to note that the anisotropy increases with the number of photons involved in the transition. This can be attributed to the sharpening of the initial alignment when all transition dipoles in a multiphoton transition are parallel to each other.

In order to express the time dependent angle between the pump dipole (at $t = 0$) and the evolving probe dipole $\eta(t)$, knowledge of the initial relative orientation between these two dipoles is necessary. The following treatment will concentrate on two particular cases, $\eta(0) = 0$ and $\eta(0) = \pi/2$. The former has a probe dipole parallel to the pump dipole at time zero; this is the ($\parallel$, $\parallel$) case. When $\eta(0) = \pi/2$, the probe dipole is perpendicular to the pump dipole at time zero; this is the ($\parallel$, $\perp$) case.

We will assume that the fragment being probed is a linear species and that its electronic and spin angular momenta are negligible compared with its rotational angular momentum. With these assumptions in mind, we can write (see Baskin and Zewail[12] for details)

$$\cos\eta_j^{\parallel,\,\parallel}(t) = \cos\omega_j t$$

$$\cos\eta_j^{\parallel,\,\perp}(t) = \cos\psi_0\,\sin\omega_j t \tag{A7}$$

where $\omega_j = 4\pi Bj$ is the rate of nutation of the fragment with a rotational quantum number j about its total angular momentum $\boldsymbol{j}$ and B is the rotational constant of the fragment. The quantity ψ_0 in eqn. (A7) denotes the initial angle about the figure axis. Substituting eqn. (A7) for the parallel case into eqn. (A6), we find the rotational anisotropy for the ($\parallel$, $\parallel$) case to be

$$r_{\parallel,\,\parallel}(j, t) = \frac{1}{2}\,\frac{m}{2m+3}\,(1 + 3\cos 2\omega_j t) \tag{A8}$$

Substitution of eqn. (A7) for the perpendicular case to eqn. (A6) and noting that averaging $\cos^2\psi_0$ over ψ_0 (from 0 to 2π) yields 1/2, we obtain the rotational anisotropy for the

(∥, ⊥) case to be

$$r_{\parallel,\perp}(j,t) = -\frac{1}{2}\frac{m}{2m+3}(1 + 3\cos 2\omega_j t) \tag{A9}$$

This final expression is very similar to eqn. (A8) except for a factor of $-1/2$. The overall reduction in alignment arises from differences in the initial population being described by $\cos^{2m}\theta$ for parallel transitions or $\sin^{2m}\theta$ for perpendicular transitions.[33]

The overall experimentally measurable rotational anisotropy $r(t)$ can be evaluated as an average of the j-dependent $r(j, t)$ in eqn. (A6), eqn. (A8), or eqn. (A9) using eqn. (A1). If the j-dependent rotational anisotropy $r(j, t)$ in eqn. (A1) is substituted with the expression in eqn. (A8) or (A9), we obtain the following expressions of rotational anisotropy for the (∥, ∥) and the (∥, ⊥) cases:

$$r_{\parallel,\parallel}(t) = \frac{1}{2}\frac{m}{2m+3} + \frac{3}{2}\frac{m}{2m+3}\frac{\sum_j P(j)\cos 2\omega_j t}{\sum_j P(j)}$$

$$r_{\parallel,\perp}(t) = -\frac{1}{4}\frac{m}{2m+3} - \frac{3}{4}\frac{m}{2m+3}\frac{\sum_j P(j)\cos 2\omega_j t}{\sum_j P(j)} \tag{A10}$$

The asymptotic limits at $t = \infty$ are $m/[2(2m + 3)]$ for the (∥, ∥) case and $-m/[4(2m + 3)]$ for the (∥, ⊥) case.

References

1 H. Okabe, in *Photochemistry of Small Molecules*, wiley, New York, 1978, pp. 73–80.
2 H. Okabe, A. H. Laufer and J. J. Ball, *J. Chem. Phys.*, 1971, **55**, 373.
3 L. J. Butler, E. J. Hintsa, S. F. Shane and Y. T. Lee, *J. Chem. Phys.*, 1987, **86**, 2051.
4 P. J. Dyne and D. W. G. Style, *J. Chem. Soc.*, 1952, 2122.
5 D. W. G. Style and J. C. Ward, *J. Chem. Soc.*, 1952, 2125.
6 G. Black, *Research on High Energy Storage for Laser Amplifiers*, Stanford Research Institute Report MP76-107, 1976.
7 H. Okabe, M. Kawasaki and Y. Tanaka, *J. Chem. Phys.*, 1980, **73**, 6162.
8 C. Fotakis, M. Martin and R. J. Donovan, *J. Chem. Soc., Faraday Trans. 2*, 1982, **78**, 1363.
9 S. R. Cain, R. Hoffmann and E. R. Grant, *J. Phys. Chem.*, 1981, **85**, 4046.
10 U. Marvet and M. Dantus, in *Femtochemistry*, ed. M. Chergui, World Scientific, Singapore, 1996, p. 134; U. Marvet and M. Dantus, *Chem. Phys. Lett.*, 1996, **256**, 57.
11 The term coherence is used here to imply that molecules share a common vibrational phase as determined by their vibrational frequency.
12 J. S. Baskin and A. H. Zewail, *J. Chem. Phys.*, submitted; Q. Zhang, U. Marvet and M. Dantus, *J. Chem. Phys.*, submitted.
13 U. Marvet, Q. Zhang, E. J. Brown and M. Dantus, manuscript in preparation.
14 J. B. Koffend, A. M. Sibai and R. Bacis, *J. Phys.* (*Paris*), **1982, 43**, 1639 and references therein.
15 J. Tellinghuisen, *J. Mol. Spectrosc.*, 1982, **94**, 231; X. Zheng, S. Fei, M. C. Heaven and J. Tellinghuisen, *J. Chem. Phys.*, 1992, **96**, 4877.
16 A. Sur and J. Tellinghuisen, *J. Mol. Spectrosc.*, 1981, **88**, 323.
17 P. C. Tellinghuisen, B. Guo, D. K. Chakraborty and J. Tellinghuisen, *J. Mol. Spectrosc.*, 1988, **128**, 268.
18 U. Heemnan, H. Knockel and E. Tiemann, *Chem. Phys. Lett.*, 1982, **90**, 17.
19 P. J. Wilson, T. Ridley, K. P. Lawley and R. J. Donovan, *Chem. Phys.*, 1994, **182**, 325.
20 R. G. Gordon, *J. Chem. Phys.*, 1966, **45**, 1643.
21 M. Kawasaki, S. J. Lee and R. Bersohn, *J. Chem. Phys.*, 1975, **63**, 809.
22 S. L. Baughcum and S. R. Leone, *J. Phys. Chem.*, 1980, **72**, 6531.
23 A. Gedanken and M. D. Rowe, *Chem. Phys.*, 1979, **36**, 181.
24 J. B. Koffend and S. R. Leone, *Chem. Phys. Lett.*, 1981, **81**, 136.
25 W. H. Pence, S. L. Baughcum and S. R. Leone, *J. Phys. Chem.*, 1981, **85**, 3844.
26 J. Tellinghuisen, *J. Quant. Spectrosc. Radiat. Transfer*, 1978, **19**, 149.
27 K. Wieland, J. B. Tellinghuisen and A. Nobs, *J. Mol. Spectrosc.*, 1972, **41**, 69.
28 K. Lawley, P. Jewsbury, T. Ridley, P. Langridge-Smith and R. Donovan, *Mol. Phys.*, 1992, **75**, 811.

29 A. L. Guy, K. S. Viswanthan, A. Sur and J. Tellinghuisen, *Chem. Phys. Lett*., 1980, **73**, 582.
30 M. Dantus, M. J. Rosker and A. H. Zewail, *J. Chem. Phys*., 1988, **89**, 6128.
31 M. Shapiro and R. Bersohn, *J. Chem. Phys*., 1986, **90**, 3644.
32 M. Shapiro, *J. Chem. Phys*., 1980, **73**, 3810.
33 R. N. Zare, *Mol. Photochem*., 1972, **4**, 1.

Paper 7/05759H; *Received* 6*th August*, 1997